Journal of Fluorescence, Vol. 15, No. 1, January 2005 (©2005)
DOI: 10.1007/s10895-005-0208-8

Spectroscopic Studies of Fluorescent Dye *N*,*N*′-bis(2-hydroxy-5-methyl-benzylidene)-1,2-ethanediamine and its DNA Complex in Solution

Lei Z. Zhang[1,3] and Guo-Qing Tang [1,2]

Received April 19, 2004; accepted August 24, 2004

Absorption and fluorescence emission properties of an *N*-salicylideneamine fluorescent dye molecule *N*,N′-bis(2-hydroxy-5-methylbenzylidene)-1,2-ethanediamine (**1**) have been studied in three typical solvents—2-methylbutane, ethanol, dimethyl sulphoxide (DMSO), and its DNA complex in methanol/H_2O mixed solvent. The normal absorption band of **1** is observed in both aprotic and protic solvents and has been assigned to the $l \rightarrow a_\pi$ transition in the enol form of **1**. The long-wavelength absorption band of **1**, which is caused by the formation of a *cis*-keto species in the ground state, is absent in aprotic solvents, but is observable in protic ones. Normal fluorescence emission from the excited enol state of **1** is obtained only when the normal absorption band is excited, while the excited-state intramolecular proton transfer (ESIPT) emissions from both *cis*- and *trans*-keto species are recorded in all cases, being acceptable for the variation of the relative emission intensities. A preliminary spectroscopic study of the **1**–DNA complex indicates an intercalation-binding mode, the convincing supporting evidence being the enhanced ESIPT fluorescence intensity of **1** when complexed with DNA. Finally, a universal energy-state diagram is given to interpret the experimental results.

KEY WORDS: *N*-Salicylideneamine; DNA; fluorescence; proton transfer.

INTRODUCTION

Proton-transfer processes are of considerable importance for research devoted to spectroscopic studies in the condensed phase with significant implications in the areas of photophysics and photochemistry [1–5]. In organic bifunctional molecules containing hydrogen-atom donor groups in close proximity to acceptor groups, an intramolecular hydrogen bond (IHB) is generally formed in the electronic ground state [6–10]. 7-Azaindole [11,12], 7-hydroxyquinoline [13,14], and 3-hydroxyflavone [15,16] are a few of the typical examples. One class of the most attractive organic molecules possessing IHBs so far is the *N*-salicylideneamine molecules [1,17,18], which are characterized by two absorption bands lying in the near-ultraviolet and the visible, respectively, in protic solvents while just one lying in the near-ultraviolet in aprotic solvents. The absorption band in the near-ultraviolet is referred to the "normal band," while the band extended to the visible is therefore specified as the "long-wavelength band" [19]. The intramolecular redistribution of electronic charge due to the photon absorption in these *N*-salicylideneamine molecules induces an elementary reorganization of the molecular structure that is generally referred to as the electronically excited-state intramolecular proton transfer (ESIPT). The most striking feature of spectroscopy in these systems is the highly-Stokes-shifted fluorescence (6000–10 000 cm^{-1}) of the product tautomer [1,6]. However, despite of the numerous reports on the

[1] Institute of Modern Optics, Nankai University, Tianjin 300071, PR China.
[2] To whom correspondence should be addressed. E-mail: gqt@nankai.edu.cn
[3] Present address: Arthur Amos Noyes Laboratory of Chemical Physics, California Institute of Technology, Pasadena, California 91125.

ESIPT emission of this class of molecules, the observation of the normal emission, which is also known as the short-wavelength emission, is less mentioned in the literature. To gain a clearer understanding of the origin of these absorption bands and consequent photoluminescence mechanisms of this kind of IHB-containing molecules, we need information concerning the initial state of the molecules involved. The primary aim of the present study is to obtain such information.

This contribution reports the absorption and photoluminescence spectra of an *N*-salicylideneamine fluorescent dye molecule, *N*,*N*′-bis(2-hydroxy-5-methylbenzylidene)-1,2-ethanediamine (**1**) in three typical solvents—2-methylbutane, ethanol, dimethyl sulphoxide (DMSO) and its DNA complex in methanol/H_2O mixed solvent (see Scheme 1 for the molecular structure diagram of **1**). It is hoped that the dependence of the spectra on solvent properties such as polarity and hydrogen-bonding ability would provide information concerning the nature of the light absorption species and the assignment of the emission bands. Moreover, a detailed elucidation of the spectroscopic properties of **1** in solution is expected to be beneficial for understanding its binding interactions with DNA, which is a unique sensitive environment for functional molecules possessing IHBs.

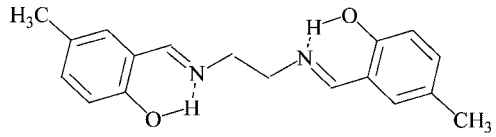

enol form **1**

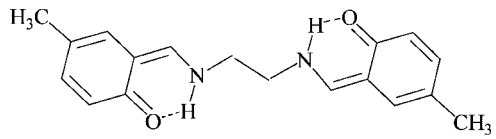

cis-keto form **1**

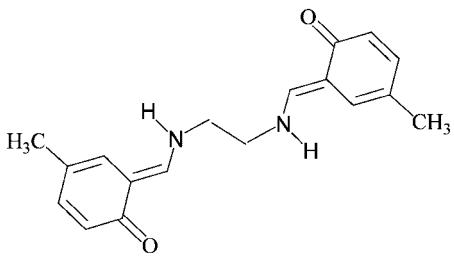

trans-keto form **1**

Scheme 1. The molecular structure diagrams for ground state of **1**.

EXPERIMENTAL

Apparatus

Elemental analyses of C, H, and N were carried out at the Institute of Elemento-Organic Chemistry, Nankai University. Infrared spectrum of **1** in the KBr disc was recorded on a Shimadzu IR-408 infrared spectrometer in the 4000–600 cm^{-1} region. UV–Visible absorption spectra of **1** in different solvents by using a quartz cell with the path length of 1.0 cm were all recorded on a Shimadzu UV-2101 spectrophotometer. Xenon arc lamp was used as the excitation light source in the measurements of emission spectra. All the emission spectra were measured on Acton Research SpectroPro-300i spectrometer with spectral CCD operating at –15°C.

Reagents

All the chemicals used in this work were of analytical reagent and used without further purification, unless otherwise stated. Double distilled water was used for solution preparation. Commercially prepared herring sperm DNA was obtained from Sigma Chemical Company and was stored at 4°C. To prepare stock solution, it was directly dissolved in water at a DNA concentration of 1 mmol/L in nucleotide phosphate, the concentration of which had been determined by absorption spectroscopy according to the literature methods [20]. Interactions of DNA with water-insoluble organic molecules were routinely studied in mixed solvent system. In this study, buffered aqueous solution of DNA was mixed with a methanol solution of **1** ($V_{methanol}/V_{H2O} = 70\%$), the final concentrations being 100 and 5 μM for DNA and **1**, respectively. The final buffer solution of pH 7.1 contained 50 mmol/L NaCl and 5 mmol/L Tris.

Sample Preparations

For the synthesis of **1**: 2-hydroxy-5-methylbenzaldehyde (1.36 g, 10 mmol) was dissolved in ethanol (5 mL) in a small flask. Ethylenediamine (0.30 g, 5 mmol) was added dropwise. Yellow powder precipitates as stirring. They were filtered off, recrystallized from ethanol and dried in air. Yield: 1.19 g (80%). IR spectrum (cm^{-1}): 1636, 1584 ($\nu_{C=N}$). Anal. Calc. For $C_{18}H_{20}N_2O_2$: C, 72.95; H, 6.80; N, 9.45; Found C, 72.41; H, 6.88; N, 9.37.

RESULTS AND DISCUSSION

Spectroscopic Studies of 1 in Solution

The absorption and photoluminescence spectra of **1** have been recorded in three solvents—2-methylbutane,

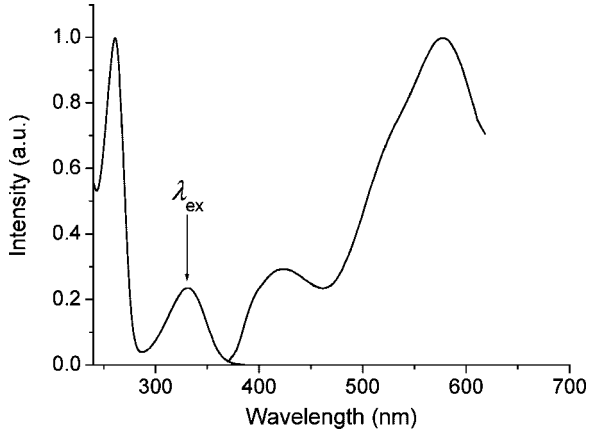

Fig. 1. The normalized absorption and photoluminescence spectra of **1** in 2-methylbutane, $\lambda_{ex} = 330$ nm.

ethanol, and DMSO in the order of increasing polarity. The latter two solvent molecules contain oxygen atoms, which are proton acceptor and are apt to the formation of intermolecular hydrogen bonds with the hydroxyl groups of **1**. There are also proton donors in ethanol, which are prone to the formation of intermolecular hydrogen bonds with the nitrogen atoms of **1**. The different physical properties of the solvents should influence the spectroscopy of **1** in the solution. The normalized absorption and emission spectra of **1** in 2-methylbutane (1.0×10^{-5} M) is presented in Fig. 1. It is generally agreed that the absorption peaks of **1** below 300 nm, no matter in what solvents, are due to the $\pi \rightarrow \pi^*$ absorption of the benzene ring, which is also confirmed by the independence of these peaks on different solvents. Despite of these bands, the absorption spectrum in this figure consists of a broad band with maximum at 330 nm (30 303 cm^{-1}, $\varepsilon_{max} = 7850$ M^{-1} cm^{-1}), which drops to zero in the vicinity of 380 nm. Essentially the same absorption feature of **1** in other aprotic solvents, such as methylcyclohexane and toluene, is also observed. Excited by 330 nm UV light, the emission spectrum of **1** is characterized by a strong broad band with maximum at 576 nm (17 361 cm^{-1}) and a weak band at about 424 nm (23 585 cm^{-1}). In addition, a very weak shoulder at about 510 nm can be detected on the fluorescence band. The presence of three emission bands, being acceptable for the variation of their relative emission intensities, has been unambiguously confirmed when recording the photoluminescence spectra of **1** in protic solvents using the same excitation wavelength as given below.

Figure 2 shows the normalized absorption and photoluminescence spectra of **1** in ethanol (1.0×10^{-4} M). Besides the $\pi \rightarrow \pi^*$ absorption bands, two bands that respectively locate at 329 nm (30 395 cm^{-1}, $\varepsilon_{max} =$

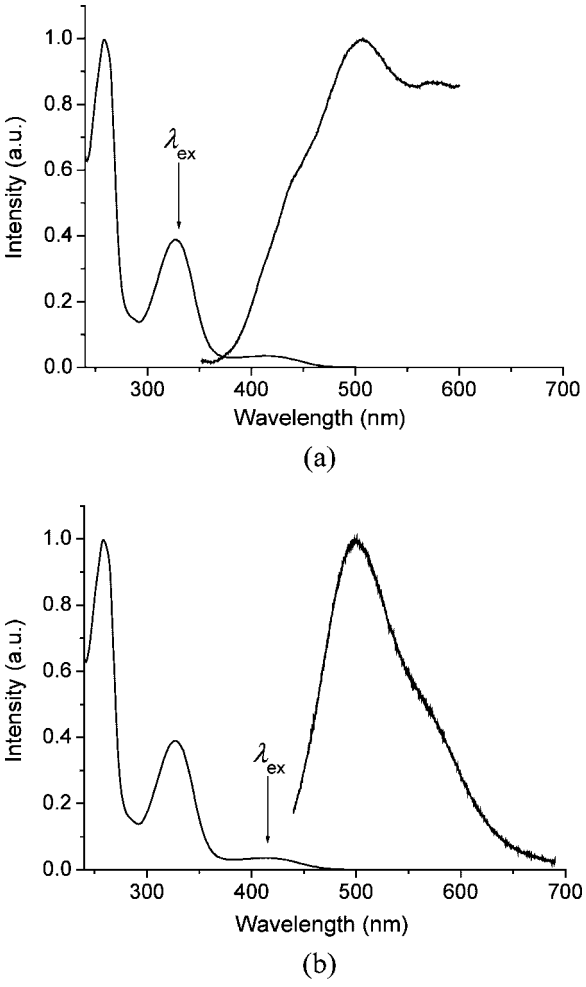

Fig. 2. The normalized absorption and photoluminescence spectra of **1** in ethanol: (a) $\lambda_{ex} = 330$ nm; (b) $\lambda_{ex} = 415$ nm.

6080 M^{-1} cm^{-1}) and 414 nm (24 155 cm^{-1}, $\varepsilon_{max} =$ 567 M^{-1} cm^{-1}) are identified in the absorption spectrum and can be specified as the normal and long-wavelength bands. Excited by 330 nm UV light, three emission bands, although varied comparing to those shown Fig. 1, are observed and displayed in Fig. 2a. This emission spectrum is characterized by a dominant peak centering at 505 nm and with two shoulder bands on both sides. Using 415 nm light excitation (see Fig. 2b), the emission spectrum of **1** is dominated by a strong emission with maximum at 499 nm (20 040 cm^{-1}) and a shoulder centered at about 578 nm (17 301 cm^{-1}).

The normalized absorption and photoluminescence spectra of **1** in DMSO (1.0×10^{-4} M) are presented in Fig. 3. The absorption below *ca*. 250 nm exhibits a cutoff drop, which is related to the solvent DMSO. The normal and long-wavelength bands are located at 328 nm

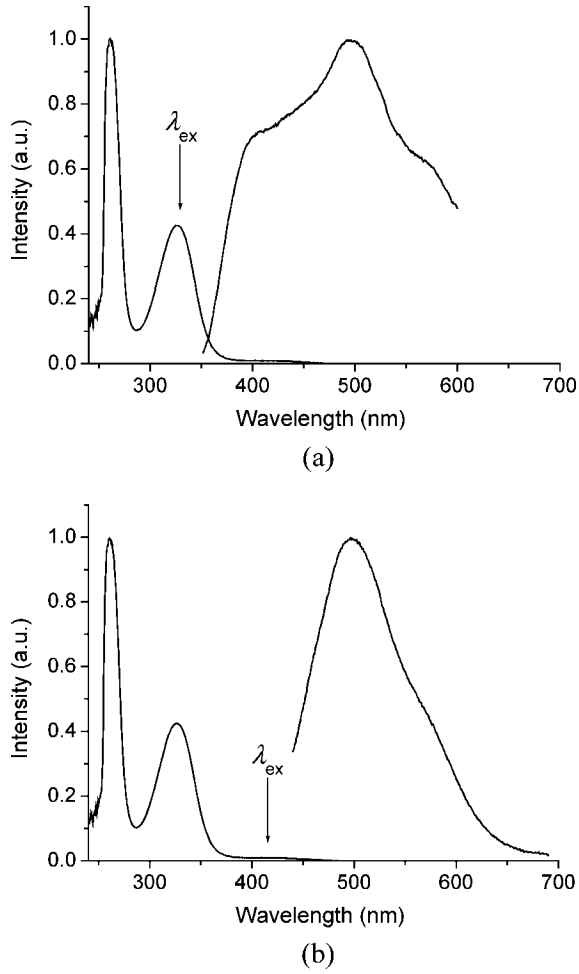

Fig. 3. The normalized absorption and photoluminescence spectra of **1** in DMSO: (a) $\lambda_{ex} = 330$ nm; (b) $\lambda_{ex} = 415$ nm.

(30 488 cm^{-1}, $\varepsilon_{max} = 7810\ M^{-1}\ cm^{-1}$) and 413 nm (24 213 cm^{-1}, $\varepsilon_{max} = 392\ M^{-1}\ cm^{-1}$), respectively, which are consistent with those observed in ethanol; however, ε_{max} of the former band is larger than that in ethanol but close to that in 2-methylbutane, and ε_{max} of the latter band is less than that in ethanol. Excited by 330 nm UV light (see Fig. 3a), the emission spectrum of **1** in DMSO is comparable with that of **1** in ethanol, despite that the short-wavelength emission band apparently becomes stronger. This phenomenon should be connected with the probable reabsorption of the long-wavelength band. Since ε_{max} of this band in DMSO is markedly smaller than that in ethanol, the emission profile of **1** in DMSO should be less affected by the reabsorption. As shown in Fig. 3b, the emission spectrum in DMSO excited by 415 nm light shows a strong emission band with maximum at 498 nm (20 080 cm^{-1}) and a shoulder at *ca.* 577 nm (17 331 cm^{-1}), which is nearly identical with that recorded in ethanol.

As a whole, the above spectroscopic measurements can be best summarized as follows: (i) in absorption spectra, the normal absorption band is present in different solvents, but the long-wavelength band is only observed in protic solvents; (ii) in photoluminescence spectra, the emission bands are dependent on the excitation wavelength, viz. the respective excitation of the normal and long-wavelength bands.

It is easy to understand that the question of the structures of **1** in solution is of interest in itself. *N*-salicylideneamine molecule can in principle adopt a variety of conformations in solution. These conformations are related to the configuration of IHB in the electronic ground state, and a further complexity may be also relevant with the possible ionization. Our interest in the spectroscopic studies of **1** in solution focuses on the assignment of the normal and long-wavelength absorption bands, and the interpretation of the consequent fluorescence mechanism. It can be easily concluded from the known crystal structures and spectroscopic arguments that only enol-form **1** exists in 2-methylbutane as well as other protic solvents (see Scheme 1 for its molecular structure diagram); in this case the long-wavelength band is absent, that is, only the normal band is observed besides the $\pi \rightarrow \pi^*$ absorption bands. In the order of increasing polarity of the solvent molecules, a noticeable blue shift of the normal bands has been observed from 30 303 cm^{-1} (2-methylbutane), via 30 395 cm^{-1} (ethanol), to 30 488 cm^{-1} (DMSO). According to Kasha's rules [21], this blue shift band arises from $l \rightarrow a_\pi$ transition of enol-form **1**. Being further evidence, we have also recorded the absorption spectrum of **1** in toluene, which has the absorption maximum at 30 211 cm^{-1}. Hence, the S_1 state of **1** should be the (l, a_π) state and the normal absorption can be best assigned to the $l \rightarrow a_\pi$ transition of **1**, which corresponds to the excitation of a lone-pair electron from the $2p_z$ orbital of the oxygen atom, to an antibonding $\pi(a_\pi)$ molecular orbital of the benzene ring (including the CN double band). It is noteworthy that both the lone-pair orbital of the oxygen atom and a_π molecular orbital of the benzene ring are antisymmetric to the molecular plane defined by the phenyl ring, which makes the $l \rightarrow a_\pi$ transition spatially allowed and the transition probability comparable to that of $\pi \rightarrow \pi^*$ transition.

It is apparent that the appearance of the long-wavelength absorption band is associated with the solvent properties. Its appearance in protic solvents is believed to result from the formation of the ground-state tautomer of **1**. According to the previous related studies, this tautomer should be best assigned to a *cis*-keto species (see Scheme 1 for its molecular structure diagram) [19,22]. In addition, the keto–enol equilibria have been determined by

proton magnetic resonance spectroscopy, which is a convincing evidence supporting the presence of the *cis*-keto tautomer [23]. It is also noteworthy that the phenomenon of the ground-state heterogeneity has been observed in some other IHB-containing molecules [24]. Obviously, the formation of the *cis*-keto tautomer is correlated with the solvent properties, which is also well reflected by the variation of the corresponding ε_{max} values of the normal and long-wavelength bands of **1** in different solvents.

Excited by 330 nm UV light, the normal emission of **1** is observed in both aprotic and protic solvents locating around 410 nm, and also two above-mentioned longer wavelength emission bands can be identified obviously, which are ascribed to the emission from the keto-form **1** after ESIPT tautomerization process. It should be mentioned that the profiles of the emission spectra could be altered due to different excited state processes and the reabsorption by the long-wavelength absorption bands appeared in the solvents. It is a convincing evidence for ESIPT that the relative intensity of the normal emission in aprotic solvent is much lower than that in protic solvent even though the reabsorption exists in the latter (see Figs. 1–3). Similar long-wavelength emission bands, despite of the variation of the peak intensities, are also observed when excited by 415 nm light. The emission band at around 500 nm is due to the emission of the *cis*-keto species of **1**. The other component, which is responsible for the even longer emission at *ca*. 577 nm, is considered to be an additional quinoid isomer of **1** but not the same species as the *cis*-keto species. By performing photochemical kinetic studies of similar salicylideneaniline molecules, Barbara *et al*. proposed that the common precursor to the both keto species is a vibrationally excited keto state [25]. Our data are consistent with this proposal and we tentatively assign a *trans*-keto species as the additional quinoid isomer of 1 (see Scheme 1 for its molecular structure diagram), which is also coincident with recent literatures [26,27].

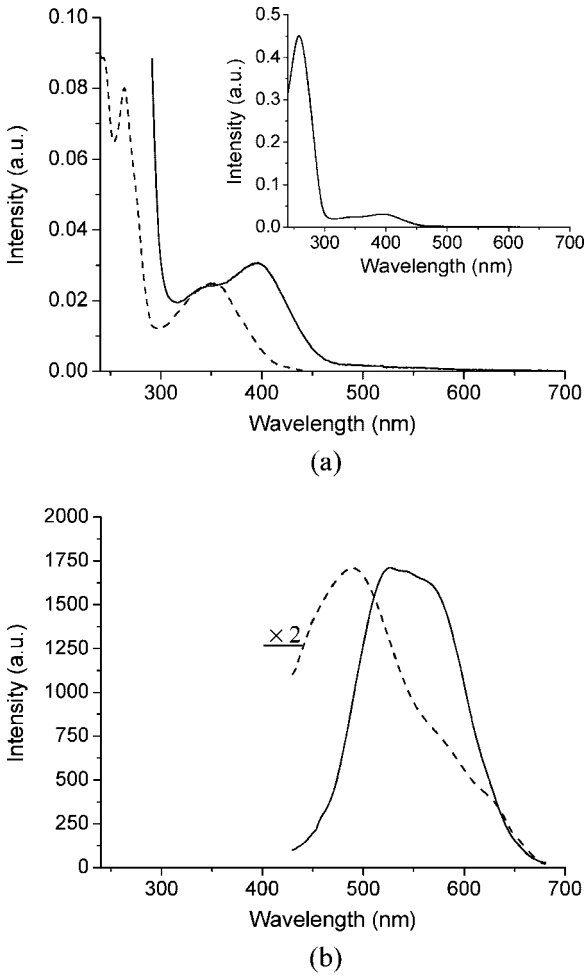

Fig. 4. (a) The absorption spectra of pure **1** (dashed line) in methanol and **1**–DNA complex (solid line) in methanol/water mixed solvent. *Inset*. The entire absorption spectrum of **1**–DNA complex. (b) The photoluminescence spectra of pure **1** (dashed line) in methanol and **1**–DNA complex (solid line) in methanol/water mixed solvent, $\lambda_{ex} = 415$ nm.

Spectroscopic Studies of 1–DNA Complex

In this contribution, we aim at presenting a preliminary spectroscopic study of the binding interactions between **1** and DNA. We hope that the studies on spectroscopic properties of **1** in solution could help us to better understand the formation of **1**–DNA complex and its spectral signatures. Figure 4a shows the absorption spectra of pure **1** in methanol (5 μM) and **1** (5 μM)–DNA (100 μM) complex in methanol/water mixed solvent system. The absorption spectrum of **1**–DNA complex displays a strong band at *ca*. 260 nm (see the inset of Fig. 4a for the entire spectrum), which exactly corresponds to that of pure DNA. The normal absorption band has been recorded in both pure **1** and its DNA complex and should be contributed by **1** only, since pure DNA aqueous solution at this concentration does not exhibit any noticeable absorption above 320 nm. A close examination of Fig. 4a reveals a faint decrease of the peak intensity of **1** (hypochromic effect) in the presence of DNA, which is suggested to be due to the interaction between the electronic states of the intercalated chromophore and DNA bases [28]. It is evident that a strong long-wavelength absorption band dominated at 395 nm appears when **1** binds to DNA, which may be in tandem with the formation of a certain species of **1**, and further studies are needed to elucidate its nature. Excited by 415 nm light, the corresponding photoluminescence spectra of pure **1** and its DNA complex are shown

in Fig. 4b. In addition to a marked change of the dominant peak position, the emission intensity of **1** complexed with DNA increases by a factor of *ca.* 2 comparing with that of pure **1**. The differences of absorption and photoluminescence spectra between pure **1** and **1**–DNA complex should be connected with the binding model of **1** to DNA.

In general, compounds and metal ion complexes of small molecules can bind nucleic acids in electrostatic, groove, and intercalation ways [29,30]. It is well known that the structure planarity and non-negative charge are two vital factors required for an efficient intercalative probe [31]. It is our contention here that the binding mode of **1** to DNA is intercalation mainly. The most convincing evidence is showcased by the results of the photoluminescence spectral measurements. As mentioned above, the remarkable increase of the emission intensity of **1** complexed with DNA is well in accordance with the fact that intercalation of IHB-containing molecule between adjacent base-pairs should enhance ESIPT as a result of lower polarity of intercalation pocket and enforced planarity of the molecule. However, the possible groove-binding mode may not be ruled out. Since the present contribution places emphasis on a preliminary spectroscopic study, further experiments are needed to confirm the exact binding mode. It should be noted that the dominant emission of **1** complexed with DNA falls into the even longer wavelength region, and therefore the emission should be ascribed to the *trans*-keto species. The variation of the emission spectrum of **1**–DNA complex comparing to that of pure **1** should be in tandem with the appearance of the strong long-wavelength absorption band of **1** when complexed with DNA.

All these above observations lead to the following energy-state diagram as shown in Fig. 5, in which radiationless processes are represented as dashed arrows. The S_1 state denotes the (l, a_π) state of **1** in enol form, which lies energetically higher than the lowest excited

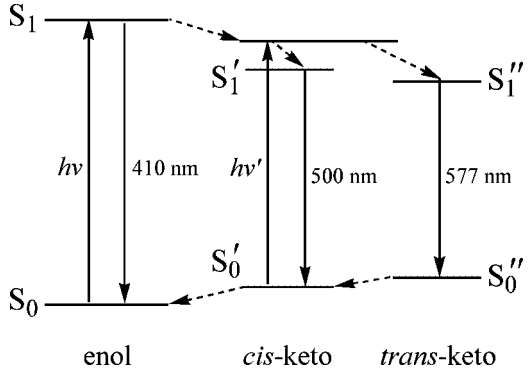

Fig. 5. Proposed energy-state diagram of **1**.

states of **1** in keto forms. Photon absorption of the enol and *cis*-keto (in protic solvents only) species are illustrated in this figure, which corresponds to the normal and long-wavelength absorption. The Franck-Condon vertically excited enol state **1** undergoes an ESIPT tautomerization process producing excited quinoid species, which contains a substantial amount of excess vibrational energy. This quinoid compound is rapidly converted to relaxed *cis*-keto species by vibrational relaxation, and is also reactive toward the formation of *trans*-keto species. Excitation of *cis*-keto **1** is followed by essentially the same vibrational energy relaxation processes, and the subsequent emission bands of the corresponding *cis*- and *trans*-keto species are observed. It should be noted here that the related *cis*-keto molecule, however, does not produce *trans*-keto molecule. This model is also well consistent with the previous fluorescence kinetic studies of similar salicylideneaniline molecules [25]. Apparently, it is easy to explain the absorption and photoluminescence spectra of **1** complexed with DNA by this energy-state model as well.

CONCLUSION

In summary, we report in this contribution the absorption and photoluminescence studies of an *N*-salicylideneamine fluorescent dye molecule, *N*,*N*′-bis(2-hydroxy-5-methylbenzylidene)-1,2-ethanediamine, in three typical solvents and its DNA complex in mixed solvent. Our present work shows that the ground-state heterogeneity of **1** is associated with the solvent properties, which results in different absorption and emission spectra of **1**. The normal absorption band has been assigned to the $l \rightarrow a_\pi$ transition and the long-wavelength band, which appears in protic solvents only, is indicative of the formation of the keto species of **1** in the ground state. Emissions from the excited enol, *cis*- and *trans*-keto states can be observed when the normal band is excited, while excitation of the long-wavelength band in protic solvents results in emissions from both keto species. A preliminary spectroscopic study of **1**–DNA complex reveals an intercalation-binding mode, the convincing evidence supporting this hypothesis being the enhanced ESIPT fluorescence intensity of **1** when complexed with DNA. Further studies of the interactions between the fluorescent probe molecules and nucleic acids are underway in our laboratory.

ACKNOWLEDGMENT

This work is supported by the Science and Technology Committee of Tianjin (Nos. 023107611 and 003101511).

REFERENCES

1. A. Douhal, F. Lahmani, and A. H. Zewail (1996). Proton-transfer reaction dynamics. *Chem. Phys.* **207**, 477–498.
2. D. Zhong, A. Douhal, and A. H. Zewail (2000). Femtosecond studies of protein-ligand hydrophobic binding and dynamics: Human serum albumin. *Proc. Natl. Acad. Sci. USA* **97**, 14056–14061.
3. T. Fiebig, M. Chachisvilis, M. Manger, A. H. Zewail, A. Douhal, I. Garcia-Ochoa, and A. de La Hoz Ayuso (1999). Femtosecond dynamics of double proton transfer in a model DNA base pair: 7-Azaindole dimers in the condensed phase. *J. Phys. Chem. A* **103**, 7419–7431.
4. R. Yang and S. G. Schulman (2001). Kinetics of excited-state proton transfer of doubly protonated 2-aminoacridine. *J. Fluoresc.* **11**, 109–112.
5. R. Yang and S. G. Schulman (2003). Proton transfer of phenanthridone in the lowest excited singlet state in moderately concentrated mineral acid solutions. *J. Fluoresc.* **13**, 89–93.
6. L. I. Krishtalik (2000). The mechanism of the proton transfer: an outline. *Biochim. Biophys. Acta* **1458**, 6–27.
7. G.-Q. Tang, J. MacInnis, and M. Kasha (1987). Proton-transfer spectroscopy of benzanilide. The amide-imidol tautomerism. *J. Am. Chem. Soc.* **109**, 2531–2533.
8. X. -M. Shang, Y. -Q. Liu, G. -Q. Tang, G. -L. Zhang, and W. -J. Chen (1998). Optical nonlinearities of hypocrellin A with the excitation of nanosecond pulses. *J. Opt. Soc. Am. B* **15**, 1502–1511.
9. T. Htun (2003). Excited-state proton transfer in nonaqueous solvent. *J. Fluoresc.* **13**, 232–239.
10. J. Jethwa, D. Ouw, K. Winkler, N. Hartmann, and P. Vöhringer (2000). Ultrafast proton-transfer and coherent wavepacket motion of electronically excited 1,8-dihydroxyanthraquinone in liquid benzyl alcohol solution. *Z. Phys. Chem.* **214**, 1367–1381.
11. J. Catalán, J. C. del Valle, and M. Kasha (1999). Resolution of concerted versus sequential mechanisms in photo-induced double-proton transfer reaction in 7-azaindole H-bonded dimer. *Proc. Natl. Acad. Sci. USA* **96**, 8338–8343.
12. D. E. Folmer, E. S. Wisniewski, S. M. Hurley, and A. W. Castleman, Jr. (1999). Femtosecond cluster studies of the solvated 7-azaindole excited state double-proton transfer. *Proc. Natl. Acad. Sci. USA* **96**, 12980–12986.
13. A. Douhal and R. Sastre (1994). Room-temperature triple proton-transfer of 7-hydroxyquinoline and stabilization of its ground-state keto tautomer in a polymer matrix. *Chem. Phys. Lett.* **219**, 91–94.
14. D. Xiao, G. -L. Zhang, H. -Y. Wang, G. -Q. Tang, and W. -J. Chen (2000). Study on dynamic optical nonlinearities of excited state proton transfer in ethanol solution of 7-hydroxyquinoline. *Chem. Phys. Lett.* **318**, 433–439.
15. D. McMorrow and M. Kasha (1984). Intramolecular excited-state proton transfer in 3-hydroxyflavone. Hydrogen-bonding solvent perturbations. *J. Phys. Chem.* **88**, 2235–2243.
16. B. J. Schwartz, L. A. Peteanu, and C. B. Harris (1992). Direct observation of fast proton transfer: Femtosecond photophysics of 3-hydroxyflavone. *J. Phys. Chem.* **96**, 3591–3598.
17. A. Mandal, D. Fitzmaurice, E. Waghorne, A. Koll, A. Filarowski, D. Guha, and S. Mukherjee (2002). Ground and excited state proton transfer reaction of two new o-hydroxy Schiff bases in some protic solvents at room temperature and 77 K. *J. Photochem. Photobiol. A* **153**, 67–76.
18. C. G. Zhang, P. Z. Zu, D. Wu, and K. B. Yu (2000). Evidence of proton transfer from the hydroxy O atom to the imine N atom, Crystal structure of *N*-salicylidene-amine-1-*tris*(hydroxymethyl)methane. *J. Chem. Res.* 402–403.
19. M. D. Cohen and G. M. J. Schmidt (1962). Photochromy and thermochromy of anils. *J. Phys. Chem.* **66**, 2442–2446, and references cited therein.
20. M. E. Reichmann, S. A. Rice, C. A. Thomas, and P. Doty (1954). A further examination of the molecular weight and size of desoxypentose nucleic acid. *J. Am. Chem. Soc.* **76**, 3047–3053.
21. M. Kasha (1968). In G. Szigeti (Ed.), *Proceedings of the International Conference on Luminescence*, Akademiaki Kiado, Budapest, Hungary.
22. R. S. Becker and W. F. Richey (1967). Photochromic anils. Mechanisms and products of photoreactions and thermal reactions. *J. Am. Chem. Soc.* **89**, 1298–1302.
23. G. O. Dudek and E. P. Dudek (1966). Spectroscopic studies of keto–enol equilibria. IX. N^{15}-substituted anilides. *J. Am. Chem. Soc.* **88**, 2407–2412.
24. X. -M. Shang, G. -L. Zhang, Y. -Q. Liu, G. -Q. Tang, and W. -J. Chen (1998). Optical nonlinearities and molecular kinetics of hypocrellin A. *J. Phys. Chem. A* **102**, 7487–7497, and references cited therein.
25. P. F. Barbara, P. M. Rentzepis, and L. E. Brus (1980). Photochemical kinetics of salicylidenaniline. *J. Am. Chem. Soc.* **102**, 2786–2791.
26. M. Ziółek, J. Kubicki, A. Maciejewski, R. Naskrêcki, and A. Grabowska (2003). Excited state proton transfer and photochromism of an aromatic Schiff base. Pico- and femtosecond kinetics of the *N,N′*-bis(salicylidene)-*p*-phenylenediamine (BSP). *Chem. Phys. Lett.* **369**, 80–89.
27. S. Mitra and N. Tamai (2003). Dynamics of photochromism in salicylideneaniline: A femtosecond spectroscopic study. *Phys. Chem. Chem. Phys.* **5**, 4647–4652.
28. E. C. Long and J. K. Barton (1990). On demonstrating DNA intercalation. *Acc. Chem. Res.* **23**, 271–273.
29. K. E. Erkkila, D. T. Odom, and J. K. Barton (1999). Recognition and reaction of metallointercalators with DNA. *Chem. Rev.* **99**, 2777–2795.
30. C. S. Chow and F. M. Bogdan (1997). A structural basis for RNA-ligand interactions. *Chem. Rev.* **97**, 1489–1513.
31. Y. -M. Hao and H. -X. Shen (2000). Application of aluminium(III) complex with salicylidene-o-aminophenol to the fluorometric determination of nucleic acids. *Spectrochim. Acta A* **56**, 1013–1020.